A Comparison of Machine Learning Techniques for the Detection of Type-4 PhotoParoxysmal Responses in Electroencephalographic Signals*

Fernando Moncada Martins[1][0000−0002−6652−9287], Víctor M. González[1][0000−0002−0937−1882], Beatriz García[2][0000−0003−1364−2603], Víctor Álvarez[3][0000−0001−5418−3031], and José R. Villar[3][0000−0001−6024−9527]

[1] Electrical Engineering Department, University of Oviedo, SPAIN
{UO245868,vmsuarez}@uniovi.es
[2] Neurophysiology Department, University Hospital of Burgos, SPAIN
bgarcialo@saludcastillayleon.es
[3] Computer Science Department, University of Oviedo, SPAIN
villarjose@uniovi.es

Abstract. Photosensitivity is a neurological disorder in which the patients' brain produces different types of abnormal electrical responses, known as Photoparoxysmal Responses (PPR), to specific visual stimuli, potentially triggering an epileptic seizure in extreme cases. The diagnosis of this condition is based on the manual analysis and detection of these discharges in their electroencephalogram. This research focuses on comparing different Machine Learning techniques for the automatic detection of Type-4 PPR (the most extreme PPR) in a real EEG dataset, after the transformation using Principal Component Analysis. Different two-class and one-class classifiers are tested, and the best performing methods for Type-4 PPR detection are 2C-KNN and DL-NN. Obtained results are compared with those achieved from a previous research, resulting in a performance increase of 15%. This system is currently in study with subjects at Burgos University Hospital, Spain.

Keywords: EEG · PPR Detection · Photoparoxysmal Responses · Photosensitivity · Epilepsy

1 Introduction

Electroencephalography (EEG) is a technique used for measuring the brain electrical activity by a set of electrodes placed on the scalp that measures the electrical discharges produced by the neurons. Because of this non-invasive quality,

* This research has been funded by the Spanish Ministry of Economics and Industry, grant PID2020-112726RB-I00, by the Spanish Research Agency (AEI, Spain) under grant agreement RED2018-102312-T (IA-Biomed), and by the Ministry of Science and Innovation under CERVERA Excellence Network project CER-20211003 (IBERUS) and Missions Science and Innovation project MIG-20211008 (INMERBOT). Also, by Principado de Asturias, grant SV-PA-21-AYUD/2021/50994.

EEG is widely used for clinical diagnosing and monitoring of different neurological disorders, e.g. Alzheimer's disease [17, 10] or epilepsy [3].

Photosensitivity is an abnormal sensitivity of the brain that provokes electrical epileptic discharges called Photoparoxysmal Responses (PPR) as a response to certain visual stimuli, like flashing lights or light reflections, response. The literature [18] has set 4 different types of PPR depending on the spreading and the waveform of the provoked discharge (see Fig. 1).The 4 types of PPR are named i) Type-1 PPR –with spikes in the occipital region–, ii) Type-2 PPR –showing spikes followed by a biphasic slow wave in occipital and parietal regions–, iii) Type-3 PPR –denoted by spikes followed by a biphasic slow wave in occipital and parietal regions and spread to frontal regions–, and iv) Type-4 PPR –characterized by generalized poly-spikes and waves–. Among them, Type-4 PPR is the most dangerous one, as it can lead to a real epileptic seizure. Besides, in real scenarios, the PPR characteristics varies from one individual to other and with several clinical variables –such as medical treatment, sleep quality, time of day, etc–, making the identification even harder.

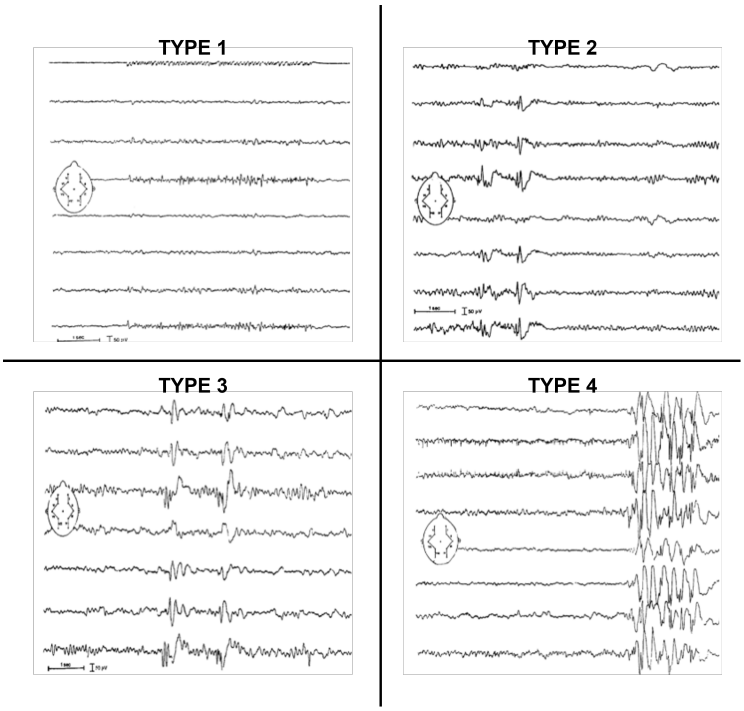

Fig. 1. The four types of PPR: **top-left** corresponds to Type-1 (spikes within the occipital rhythm); **top-right** corresponds to Type-2 (parieto-occipital spikes with biphasic slow wave); **bottom-left** corresponds to Type-3 (parieto-occipital spikes with biphasic slow wave and spread to the frontal region); **bottom-right** corresponds to Type-4 (generalized spikes and waves).

This study is a continuation of a previous study in [9], comparing different Machine Learning (ML) techniques for the automatic detection of Type-4 PPR in EEG recordings from patients who have been clinically diagnosed with photosensitivity disorder with different intensity. The final goal is to find the best method to detect the different types of PPR in order to design an automatic PPR detection system than can be used in clinical procedures.

The structure of this study is as follows. The next section focuses on some preliminaries knowledge and the related work the automated PPR detection. Section 3 describes the modelling alternatives considered in this research, detailing the different methods. Section 4 gives details of the experimentation set-up that has been carried out, while Section 5 includes all the obtained results and the discussion on them. The final section draws the conclusion of this research.

2 Preliminaries and related work

Photosensitivity evaluation is diagnosed using the Intermittent Photic Stimulation (IPS) [8, 12], where the patient -monitored with EEG- is stimuled with flashing lights at different frequencies, increasing first and decreasing later, so to detect the frequency thresholds where the individual is sensitive. The detection and analysis of PPR is carried out manually by the clinical neurophysiologists and nurses, who perform a visual inspection of the patient's whole EEG recording searching these phenomena while taking into account their clinical context.

To our best knowledge, no automated method for the detection of PPR using the standard stimulation system has been developed so far. [14] designed a PPR detection method by analysing the brain response provoked by a flashing stimulation, but following a different stimulation pattern from the standard IPS used in clinical diagnosis. There are other recent studies that analyse the photosensitivity and epilepsy based directly on generalized seizures: in [11], a detection method based on the fluctuation from a high-frequency and a low-frequency components in each EEG channel is proposed; [16] applied the Extreme Gradient Boost technique for the classification of seizures, while a channel-independent Long Short-Term Memory Network is used in [2]; the combined information extracted from both EEG and electrocardiogram (ECG) signals is used in [20] in a multi-modal Neural Network; in [3], K-Nearest Neighbours and Artificial Neural Networks are used for the detection of ictal discharges and inter-ictal states; [19] proposed an EEG single-channel analysis applying three types of visibility graphs to represent different EEG patterns. Other studies make use of additional and different biometric measures for the same purpose, such as ECG [5, 6, 15], electromyograms (EMG) [1, 21] or magnetoencefalograms (MEG) [13].

In our previous study [9], which was published in the Neural Computing and Applications journal, a proof of concept about Type-4 PPR detection was proposed. The PPR detection task was performed by two classifiers: an unsupervised 1C-KNN and a supervised 2C-KNN. 1C-KNN classified the EEG windows as normal or abnormal and 2C-KNN classified only the abnormal windows as PPR or not. For that purpose, the EEG recordings were divided into two sets:

the first one included all the EEG windows before the first PPR of the current subject labelled as normal an was used for the 1C-KNN training; the second one was formed by normal and PPR windows from the other subjects and was used for the 2C-KNN training. This process is shown in Fig.2.

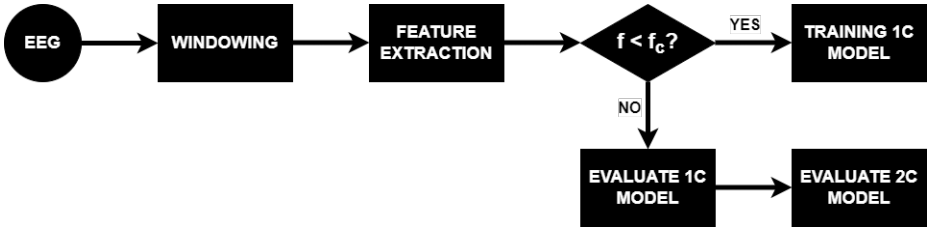

Fig. 2. When a EEG window comes from frequencies smaller than the stimulation frequency value at which the first PPR appears (fc, the cut frequency), the window is preserved for the training of the one-class models; otherwise, the window is labeled as normal or as anomaly. In this latter case, the two-class classifier labels then the anomaly window as PPR or not.

This ML procedure was used in the analysis of the effects of Virtual Reality in photosensitivity. The exposure of photosensitive and epilepsy patients to digital activities and environments has become a major concern with the huge proliferation of this technology in the last years [4].

3 Type-4 PPR detection using ML

The process we propose are designed following the steps shown in Fig.3. For this study, we focused in channel Fz because is one of the EEG channels where PPRs express themselves best.

Firstly, sliding windows of 1-second length and 90% overlapping were extracted from the raw Fz channel and preprocessed (mean subtraction and Band-Pass Butterworth Filter in the range 1-45 Hz). Due to the high imbalance of the original data (only 3% of EEG windows are PPR), undersampling is computed to reduce it, reaching a PPR ratio of 10%. Then, a dimensional reduction step is performed, where a set of transformations and features are extracted from the EEG windows and Principal Component Analysis (PCA) algorithm is used to reduce the dimensions even more. The resulting components are grouped into clusters and finally analysed and classified by ML algorithms as normal or Type-4 PPR window.

This procedure is detailed in the next sections: the dimensional reduction process is detailed in subsection 3.1 and the following clustering of the reduced data and the selection and configuration of the ML models are explained in subsection 3.2.

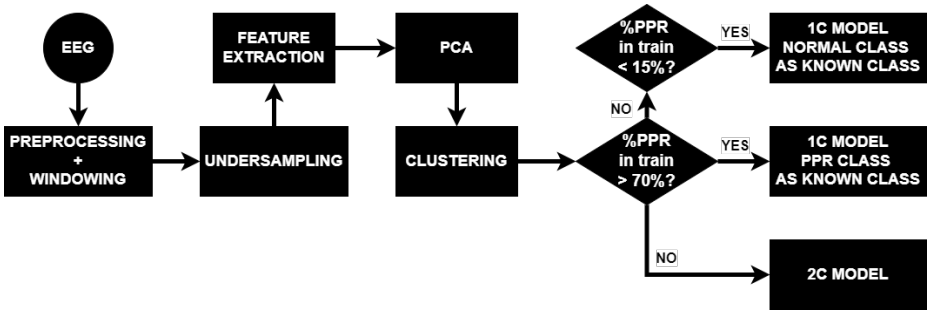

Fig. 3. The workflow of the designed experiment. The original EEG data are preprocessed and windowed and the imbalance of the data is reduced by using undersampling. The features are extracted from each EEG window. PCA and K-means are computed for dimensional reduction and clustering respectively. Depending on the proportion of PPR windows within each cluster, a different classification model is chosen.

3.1 Dimensional Reduction

Depending on the sampling rate used in the EEG recordings, the windows could include a large number of samples, which could make the tasks of the classifiers more difficult. Moreover, finding variables that present significant differences between the normal brain activity and the PPR windows could make the detection easier. Because of that, this step is focused in dimensional reduction of the processed EEG signal. A total of 32 features from temporal, statistical and spectral domains are extracted from each window.

- **Temporal Domain**: Sum of Absolute Values, Maximum Difference, Sum of Absolute Differences, Total Energy, Absolute Energy, Area Under the Curve, Entropy and Autocorrelation.
- **Statistical Domain**: Kurtosis, Skewness, Standard Deviation, Variance, Maximum, Minimum, Mean of Absolute Deviation, Root Mean Square.
- **Spectral Domain**: Fundamental Frequency, Maximum Frequency, Median Frequency, Maximum Power Spectrum, Centroid, Decrease, Spread, Distance, Skewness, Entropy, Kurtosis, Positive Turning, Roll-Off, Roll-On, Variation, Bandwith, Human Range Energy.

A cross-correlation vector between each feature and the real labels allows to find the most relevant and representative of Type-4 PPR features, which turned out to be Spectral Distance, Maximum Difference or Standard Deviation, among others. Then, a cross-correlation matrix between all features allows to analyze their independence: the correlation value is extremely high between the best features, which means that the represent the Type-4 PPR equally well.

Then, PCA algorithm is computed to reduce these 32 features into a even smaller set. PCA is the most widely used dimension-reducing technique [7]. This method extracts uncorrelated linear combinations from the initial dataset called

Principal Components, which have the maximum variance possible of the original data.

3.2 Clustering and Classification

Clustering is a ML technique that divides samples into different groups based on their similarity. After the feature extraction and the dimensional reduction performed by PCA, the new transformed set presents higher distinctions between normal and PPR windows, so grouping the data into clusters allows to distinguish better between the different classes. This step is performed by K-means algorithm after dividing the data into training set and test set. Given the training data, K-means algorithm is used to create the appropriate number of clusters (following the "elbow rule"), and testing data are then associated to the most suitable cluster.

Once the data are divided into the clusters, the proportion of PPR samples within the training data of each cluster is calculated. Depending on this value, the training and testing data of each cluster are used in a different Machine Learning technique following these rules:

- If the proportion of PPR samples within the cluster is lower than 15%, i.e., the normal class clearly predominates the cluster, a one-class (1C) classifier will be used and the normal class will be considered as the known class, training the model only with the normal samples.
- On the contrary, if the proportion of PPR samples within the cluster is higher than 75%, it will mean that the PPR class clearly predominates the cluster and a 1C classifier where the PPR class will be considered as the known class will be used, training the model only with the PPR samples.
- If the proportion of PPR samples within the cluster is in the range 15%-75%, a two-class (2C) classifier will be used and the model will be trained with all the cluster's training data.

The Machine Learning algorithms selected for this study were one-class K-Nearest Neighbours (1C-KNN) and one-class Support Vector Machine (1C-SVM) as the one-class classifiers; and two-class K-Nearest Neighbours (2C-KNN), two-class Support Vector Machine (2C-SVM), Random Forest (RF) and Neural Network with Dense Layer as the hidden layer (DL-NN) as the two-class classifiers.

4 Materials and Methods

This section introduces the data set used in this research and describes the design of the experiments. The whole process was implemented in Python.

4.1 Data Set Description

The dataset used in this research has been gathered from Burgos University Hospital. It includes ten anonymized EEG recorded sessions from different photosensitive patients recorded with the hospital's own equipment. Among these

patients, four did not present Type-4 PPR but many PPR from the other categories, so they were excluded from this study.

Each session consisted of a continuous recording while the first half of the conventional IPS procedure was performed: the frequency of the stimulation was only increased in the range 1-50 Hz, but the half corresponding to the descending frequencies half was not included. The duration of each session varies in the range 3-5 minutes. The EEG signals were recorded at a sampling rate of 500 Hz from 19 electrodes placed following the 10-20 standardized system, as shown in Fig.4.

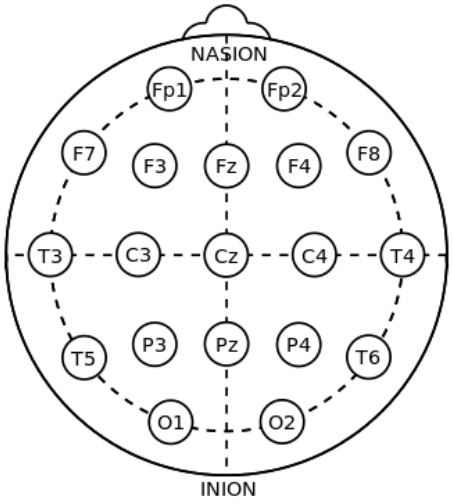

Fig. 4. Position of the 19 scalp electrodes used to record EEG signals according to the international 10–20 system of electrode placement, where Nasion is located at the center of the frontonasal area and the Inion in located at the posterioinferior part of the skull.

The selected EEG recordings were manually labelled by visual analysis, marking every PPR that can be categorized as Type-4. The proportion of both class instances within the dataset is showed in Table 1.

Nº Windows	Nº Normal Windows		Nº PPR Windows	
20130	19510	**96'92%**	620	**3'08%**

Table 1. Distribution of instances for each class within the original dataset.

4.2 Experimentation Design

For this experiment, a leave-one-out 10-fold Cross-Validation scheme is used (90% train + 10% test) with two different sets of 9 and 12 components created by PCA algorithm after reducing the set of 32 extracted features (corresponding to the 90% and 95% of the variance respectively). Both sets are used for the following process independently.

Once the data of each fold are divided into the respective fold's clusters, the proportion of PPR samples within the training data of each cluster is calculated, the corresponding classification algorithms are executed using the cluster's data and each classifier is trained and evaluated with the train data and the test data associated to its cluster, following the rules previously explained.

For each classifier, different parameter values are also tested:

- For KNN algorithm, the K number of nearest neighbours tested are 3, 5, 7, 9 and 11.
- For SVM algorithm, the parameters to be tested are the regularization parameter C and the kernel coefficient γ. The values tested are C = [0.1, 1, 10, 100, 1000] and γ = [1, 0.1, 0.01, 0.001, 0.0001]
- For DL-NN, the N number of neurons of the hidden layer tested are 10, 20, 30, 40 and 50. The number of neurons of input and output layers have been fixed to the number of input variables and 1, respectively.
- For RF, the T number of trees tested are 100, 200, 300, 400 and 500; and as for the depth of the trees, the number of L levels tested are 5, 6, 7 and 8.

To measure the performance of the different classification techniques, the Accuracy (*Acc*), the Sensitivity (*Sens*), and the Specificity (*Spec*) measurements will be calculated.

5 Results and Discussion

The results gathered in this research consist of the Acc, Sens and Spec values of all classifiers applied in each cluster into which each fold is divided and with each of the proposed parameter values. Since there are multiple combinations of algorithms with their results, Table 2 shows the best Acc, Sens and Spec values obtained in each fold by each classifier: the upper table corresponds to the one-class classifiers applied in the class-dominant clusters and the lower table corresponds to the two-class classifiers applied in the balanced clusters.

The shown results are just one example of the best-performing case. Analyzing the overall results of all classifiers, on the one hand, the results from the one-class classifiers reveal that both of these methods are not the most suitable ones for this procedure: 1C-KNN method presents high *Sens* but low *Spec* values, which means that it tends to label the new data as outliers from the known normal class; on the contrary, 1C-SVM method presents high *Spec* and low *Sens* values, which means that it cannot distinguish the PPR class from the

	1C-KNN			1C-SVM		
P_i	Acc	Sens	Spec	Acc	Sens	Spec
P_1	0.5175	0.8462	0.4255	0.7339	0.3077	0.8750
P_2	0.3634	0.5353	0.4276	0.7716	0.1087	0.8750
P_3	0.5846	0.8542	0.5306	0.6648	0.1667	1.0000
P_4	0.3208	0.6389	0.5206	0.6038	0.1042	1.0000
P_5	0.4910	0.7667	0.6280	0.8840	0.1667	1.0000
P_6	0.4590	0.7321	0.4245	0.7680	0.2500	1.0000
P_7	0.4605	0.6571	0.4367	0.7503	0.2387	1.0000
P_8	0.4732	0.6727	0.6796	0.7943	0.3824	0.5833
P_9	0.4621	0.8125	0.3377	0.8048	0.3125	0.9176
P_{10}	0.4192	0.6489	0.5523	0.7399	0.2426	1.0000

	2C-KNN			2C-SVM			RF			DL-NN		
P_i	Acc	Sens	Spec	Acc	Sens	Spec	Acc	Sens	Spec	Acc	Sens	Spec
P_1	0.7089	0.6279	0.8056	0.7342	0.6279	0.8611	0.7342	0.6279	0.8611	**0.7722**	**0.6977**	**0.8611**
P_2	0.7500	0.6786	0.7917	0.7500	0.6071	0.8333	0.7763	0.6071	0.8750	**0.7763**	**0.6786**	**0.8333**
P_3	0.7703	0.7576	0.7805	0.7973	0.6970	0.8780	0.8243	0.6970	0.9268	**0.8243**	**0.6970**	**0.9268**
P_4	**0.8028**	**0.8636**	**0.7755**	0.8028	0.7273	0.8367	0.8028	0.7727	0.8163	0.7465	0.7727	0.7347
P_5	**0.8250**	**0.7561**	**0.8974**	0.7875	0.6829	0.8974	0.8375	0.7073	0.9744	0.8000	0.7561	0.8462
P_6	0.8219	0.8276	0.8182	0.7671	0.7931	0.7500	**0.8356**	**0.8276**	**0.8409**	0.7808	0.8276	0.7500
P_7	**0.7711**	**0.7692**	**0.7727**	0.7831	0.6923	0.8636	0.7590	0.7179	0.7955	**0.7711**	**0.7692**	**0.7727**
P_8	0.6944	0.6061	0.7692	0.6944	0.6970	0.6923	0.7361	0.6364	0.8205	**0.7361**	**0.6667**	**0.7949**
P_9	**0.8462**	**0.8649**	**0.8333**	0.8571	0.8378	0.8704	0.8352	0.8378	0.8333	0.8352	0.8649	0.8148
P_{10}	**0.7831**	**0.6857**	**0.8542**	0.7831	0.6571	0.8750	0.7711	0.6286	0.8750	0.7711	0.7143	0.8125

Table 2. Best Type-4 PPR detection results of each ML algorithm proposed in each fold. The upper table corresponds to the one-class classifiers (1C-KNN and 1C-SVM), while the lower table corresponds to the two-class classifiers (2C-KNN, 2C-SVM, RF, DL).

known normal class. The higher *Acc* values from 1C-SVM are due to the data imbalance.

On the other hand, the two-class algorithms present *Acc* and *Sens* values in the range 60%–80% and *Spec* values in the range 70%–90% for various parameter values. These results are higher than the one-class ones, which means that they are able to distinguish both classes better. Moreover, the parameter values that produce the best detection performance for each classifier are the following ones: K = 3-5 for 1C-KNN, $\gamma = 0.0001$ for 1C-SVM, $K = 9$ for 2C-KNN, $C = 1$ and $\gamma = 0.01$ for 2C-SVM, T = 100-200 and L = 5-6 for RF, and N = 20-30 for DL-NN.

If the class imbalance of the data is taken into account, which makes *Spec* measure easier to raise than *Sens*, the best performing methods for Type-4 PPR detection are 2C-KNN and DL-NN.

6 Conclusions and Future Work

In this research, we compared different ML algorithms for Type-4 PPR detection. For this purpose, a set of 32 features from time, spectral and statistical domains was extracted from EEG windows and PCA technique was applied for dimensional reduction. Then, the instances were divided into clusters and a certain set of classifiers was used in each cluster according to the proportion of PPR samples within the cluster: 1C-KNN and 1C-SVM were applied in those clusters in which one class was predominant; otherwise, 2C-KNN, 2C-SVM, RF and DL-NN were used.

The ML results show that two-class classifiers can detect Type-4 PPR better than one-class classifiers, and among them, the best detection algorithms are 2C-KNN and DL-NN. Furthermore, comparing this procedure with the one tested in our previous research [9], the Type-4 PPR detection performance has been increased by around 15%, but it is not as high as expected and there is still room for improvement.

Due to the lack of a large and appropriate EEG dataset, the results are not good enough by employing classic ML algorithms. Improving the results of this research would be possible by artificially increasing the available dataset through data augmentation techniques, which allow creating more EEG recordings with Type-4 PPRs from those currently available. Re-evaluating the procedure proposed in this study with the new data may allow determining whether a plausible solution can be found using classical ML.

In addition, Deep Learning techniques can also be tested along with the data augmentation technique, such as the classification of time series using LSTM-RNN (Recurrent Neural Networks) or an autoencoder. All of these proposals represent future research work.

References

1. Beniczky, S., Conradsen, I., Henning, O., Fabricius, M., Wolf, P.: Automated real-time detection of tonic-clonic seizures using a wearable emg device. Neurology **90** (2018). https://doi.org/10.1212/WNL.0000000000004893
2. Chakrabarti, S., Swetapadma, A., Pattnaik, P.K.: A channel independent generalized seizure detection method for pediatric epileptic seizures. Computer Methods and Programs in Biomedicine **209**, 106335 (9 2021). https://doi.org/10.1016/j.cmpb.2021.106335, https://linkinghub.elsevier.com/retrieve/pii/S0169260721004090
3. Choubey, H., Pandey, A.: A combination of statistical parameters for the detection of epilepsy and eeg classification using ann and knn classifier. Signal, Image and Video Processing **15** (2021). https://doi.org/10.1007/s11760-020-01767-4
4. Fisher, R.S., Acharya, J.N., Baumer, F.M., French, J.A., Parisi, P., Solodar, J.H., Szaflarski, J.P., Thio, L.L., Tolchin, B., Wilkins, A.J., Kasteleijn-Nolst Trenité, D.: Visually sensitive seizures: An updated review by the epilepsy foundation. Epilepsia **n/a**(n/a) (Feb 2022). https://doi.org/10.1111/epi.17175, https://doi.org/10.1111/epi.17175

5. Jahanbekam, A., Baumann, J., Nass, R.D., Bauckhage, C., Hill, H., Elger, C.E., Surges, R.: Performance of ecg-based seizure detection algorithms strongly depends on training and test conditions. Epilepsia Open **6** (2021). https://doi.org/10.1002/epi4.12520
6. Jeppesen, J., Fuglsang-Frederiksen, A., Johansen, P., Christensen, J., Wüstenhagen, S., Tankisi, H., Qerama, E., Hess, A., Beniczky, S.: Seizure detection based on heart rate variability using a wearable electrocardiography device. Epilepsia **60**, 2105–2113 (10 2019). https://doi.org/10.1111/epi.16343
7. Jolliffe, I.T.: Principal component analysis, second edition. Encyclopedia of Statistics in Behavioral Science **30** (2002). https://doi.org/10.2307/1270093
8. Kasteleijn-Nolst Trenite, D.: Photosensitivity and Epilepsy, pp. 487–495. Springer International Publishing, Cham (2019). https://doi.org/10.1007/978-3-030-04573-9_29, https://doi.org/10.1007/978-3-030-04573-9_29
9. Moncada, F., Martín, S., González, V.M., Álvarez, V.M., García-López, B., Gómez-Menéndez, A.I., Villar, J.R.: Virtual reality and machine learning in the automatic photoparoxysmal response detection. Neural Computing and Applications (Jan 2022). https://doi.org/10.1007/s00521-022-06940-z, https://doi.org/10.1007/s00521-022-06940-z
10. Morrison, C., Rabipour, S., Taler, V., Sheppard, C., Knoefel, F.: Visual event-related potentials in mild cognitive impairment and alzheimer's disease: A literature review. Current Alzheimer Research **16**(1), 67–89 (Dec 2018). https://doi.org/10.2174/1567205015666181022101036, http://www.eurekaselect.com/166483/article
11. Omidvarnia, A., Warren, A.E., Dalic, L.J., Pedersen, M., Jackson, G.: Automatic detection of generalized paroxysmal fast activity in interictal eeg using time-frequency analysis. Computers in Biology and Medicine **133** (2021). https://doi.org/10.1016/j.compbiomed.2021.104287
12. Rubboli, G., Parra, J., Seri, S., Takahashi, T., Thomas, P.: Eeg diagnostic procedures and special investigations in the assessment of photosensitivity. Epilepsia **45**(5), 35–39 (2004). https://doi.org/10.1111/j.0013-9580.2004.451002.x, https://doi.org/10.1111/j.0013-9580.2004.451002.x
13. Soriano, M.C., Niso, G., Clements, J., Ortín, S., Carrasco, S., Gudín, M., Mirasso, C.R., Pereda, E.: Automated detection of epileptic biomarkers in resting-state interictal meg data. Frontiers in Neuroinformatics **11** (2017). https://doi.org/10.3389/fninf.2017.00043
14. Strigaro, G., Gori, B., Varrasi, C., Fleetwood, T., Cantello, G., Cantello, R.: Flash-evoked high-frequency eeg oscillations in photosensitive epilepsies. Epilepsy Research **172** (2021). https://doi.org/10.1016/j.eplepsyres.2021.106597
15. Ufongene, C., Atrache, R.E., Loddenkemper, T., Meisel, C.: Electrocardiographic changes associated with epilepsy beyond heart rate and their utilization in future seizure detection and forecasting methods. Clinical Neurophysiology **131** (2020). https://doi.org/10.1016/j.clinph.2020.01.007
16. Vanabelle, P., Handschutter, P.D., Tahry, R.E., Benjelloun, M., Boukhebouze, M.: Epileptic seizure detection using eeg signals and extreme gradient boosting. Journal of Biomedical Research **34** (2020). https://doi.org/10.7555/JBR.33.20190016
17. Vecchio, F., Miraglia, F., Alù, F., Menna, M., Judica, E., Cotelli, M., Rossini, P.M.: Classification of alzheimer's disease with respect to physiological aging with innovative eeg biomarkers in a machine learning implementation. Journal of Alzheimer's Disease **75**, 1253–1261 (2020). https://doi.org/10.3233/JAD-200171, https://doi.org/10.3233/JAD-200171, 4

18. Waltz, S., Christen, H.J., Doose, H.: The different patterns of the photoparoxysmal response - a genetic study. Electroencephalography and Clinical Neurophysiology **83** (1992). https://doi.org/10.1016/0013-4694(92)90027-F
19. Wang, L., Long, X., Arends, J.B., Aarts, R.M.: Eeg analysis of seizure patterns using visibility graphs for detection of generalized seizures. Journal of Neuroscience Methods **290** (2017). https://doi.org/10.1016/j.jneumeth.2017.07.013
20. Yang, Y., Truong, N., Maher, C., Kavehei, O., Truong, N.D., Eshraghian, J.K., Nikpour, A.: A multimodal ai system for out-of-distribution generalization of seizure detection (2021). https://doi.org/10.1101/2021.07.02.450974, https://doi.org/10.1101/2021.07.02.450974
21. Zibrandtsen, I.C., Kidmose, P., Kjaer, T.W.: Detection of generalized tonic-clonic seizures from ear-eeg based on emg analysis. Seizure **59** (2018). https://doi.org/10.1016/j.seizure.2018.05.001